

Investigation of electrohydrodynamic calculations

Stefan A. Bošković¹, Aleksandar Karač², Slobodan B. Vrhovac³, Aleksandar Belić³ and Branko Bugarski⁴

¹Innovation Center of the Faculty of Technology and Metallurgy in Belgrade, Belgrade, Serbia

²Polytechnic Faculty, University of Zenica, Zenica, Bosnia and Herzegovina

³University of Belgrade, Institute of Physics Belgrade, Belgrade, Serbia

⁴University of Belgrade, Faculty of Technology and Metallurgy, Belgrade, Serbia

Abstract

A perfect dielectric model was incorporated into the OpenFOAM® software and used for investigation and, possibly, improvements of electrohydrodynamic calculations. Two different sets of numerical simulations were analyzed, in which two different fluids were present. The first set was one-dimensional, while in the second, a drop of one fluid was surrounded by the other fluid. It is shown that oscillations and possible artificial generation of a curl of the electric field strength can be observed at applying certain expressions or calculation strategies, which can be thus abandoned. Usage of dynamic meshes, at least those present in the used software, and of limiters for the gradient of the electric field strength can lead to large numerical errors. It is also shown that usage of certain cell face values could improve the results. An electric Courant number was derived by dimensional analysis, and it could be suggested for future calculations. Conclusions made in this paper are expected to be transferable to other more complicated models.

Keywords: electrohydrodynamics; OpenFOAM®; perfect dielectric model; electric Courant number.

Available on-line at the Journal web address: <http://www.ache.org.rs/HI/>

ORIGINAL SCIENTIFIC PAPER

UDC: 676.017.57:537.226+53.
082.25-047.58

Hem. Ind. 76 (2) 65-74 (2022)

1. INTRODUCTION

The part of physics that tries to explain motion of a liquid in a presence of an electric field is called electrohydrodynamics (EHD) [1]. The relevant literature, ranging from books (*e.g.* [2]) to scientific articles, can be found for maybe a century or so. There is a decent number of processes that use the electric field to influence fluids [3,4], such as electrocoalescence [5], electrospraying [6] and solvent extraction. Furthermore, for example, the electrospray process is used in mass spectrometry [7], inkjet printing [8], encapsulations [9], *etc.* Despite the fact that both theoretical concepts and practical applications exist, numerical implementations of those theories are still surprisingly limited in the number [10].

In previous experimental [11-15] and theoretical [16] works, the electric field was used in the electrostatic extrusion process for obtaining small diameter particles by affecting the size of droplets that form at the end of a needle. In order to aid the experimental design and improve efficiency and cost-effectiveness of modeling involved processes, it is needed to develop fast, efficient and precise calculation methodologies. The software platform OpenFOAM® (OpenFOAM Foundation, UK) was found to be suitable for this purpose and was used in the present work.

The general approach to EHD calculations is to take into account both polarization of molecules and ohmic conduction in considered fluids [1]. Fluids in which only polarization effects are present are called perfect dielectric fluids [1]. The perfect dielectric model (*e.g.* [17,18]) is suitable as a starting point for numerical calculations because of its simplicity and possibilities for simple adjustments of starting numerical parameters. Other more complicated models can be later added by expanding the present numerical approach. It could be also noted that it is questionable whether fluids should be treated as perfect dielectrics or as perfect conductors (see *e.g.* [19,20]).

Corresponding authors: Stefan A. Bošković, Innovation Center of the Faculty of Technology and Metallurgy in Belgrade, Serbia

E-mail: sboskovic@tmf.bg.ac.rs

Paper received: 10 November 2021; Paper accepted: 16 April 2022; Paper published: xx May 2022.

<https://doi.org/10.2298/HEMIND211110010B>



The standard set-up for testing quality, stability and efficiency of the perfect dielectric model is to consider a drop of one fluid surrounded by another fluid in presence of electric field causing a deformation of the drop, as in [17]. To address this benchmark calculation, in the present study Computational Fluid Dynamics (CFD), implemented in the OpenFOAM® (version 8) software, was used. This software uses the Finite Volume Method (FVM) [21] and the Volume of Fluid (VoF) method [22], while the interface reconstruction can be carried out by, for example, the Interface Compression (IC) scheme (*e.g.* [23]). This paper reports on the results obtained by expanding an already present solver in the software (termed *interFoam*) for two immiscible and incompressible fluids and constant temperature, which uses the VoF method.

The paper is organized as follows: first the mathematical model comprising different expressions for the dielectric force and other parameters is presented, after which a set of the most promising expressions is determined, including the one-dimensional set-up and the set-up with a drop. The obtained results are appropriately discussed in order to investigate possible improvements to EHD calculations.

2. MATHEMATICAL MODEL

Since the FVM and VoF methods were used in the starting solver, they were also used in the present model. Implementation of the Navier-Stokes equation that is used in the starting solver (*cf.* [24]) was expanded by adding electric forces:

$$\frac{\partial(\rho\mathbf{U})}{\partial t} + \nabla \cdot (\rho\mathbf{U}\mathbf{U}) - \nabla \cdot (\mu\nabla\mathbf{U}) = \rho\mathbf{g} - \nabla\rho + \mathbf{F}_s + \mathbf{F}_c + \mathbf{F}_{\text{oeI}} \quad (1)$$

where ρ is the density, \mathbf{U} is the velocity vector, t is the time, μ is the dynamic viscosity, \mathbf{g} is the gravitational acceleration, ρ is the pressure, \mathbf{F}_s is the surface tension force, \mathbf{F}_c is the Coulombic force, and \mathbf{F}_{oeI} are other electric forces. Implementation of \mathbf{F}_s that was already present in the starting solver was not modified (see *e.g.* [25]). For \mathbf{F}_{oeI} , either an expression for the dielectric force (\mathbf{F}_{diel}), or the sum of expressions for the electrostrictive (\mathbf{F}_{els}) and the dielectric force could be used. This corresponds to the Korteweg-Helmholtz approach [26]. For the perfect dielectric model, \mathbf{F}_c is a zero vector, but straightforwardness of transition into other more complicated models can be seen by its inclusion. In this investigation, \mathbf{F}_{els} was neglected. The expansion was carried out in a way so that in a single time step calculation of newly added variables is finished just before calculation of the velocity and the pressure field is started.

Equations that are used for the dielectric and the electrostrictive forces are derived in literature based on the Maxwell stress tensor (\mathbf{T}_e) (*e.g.* [19]). The equation that is used for this tensor should be somewhat simplified for the perfect dielectric model (*cf.* [19]; *cf.* [1]):

$$\mathbf{T}_e = -\frac{1}{2}\varepsilon|\mathbf{E}|^2\mathbf{I} + \frac{1}{2}\rho\left(\frac{\partial\varepsilon}{\partial\rho}\right)_T|\mathbf{E}|^2\mathbf{I} \quad (2)$$

where ε is the electric permittivity, \mathbf{E} is the electric field strength, \mathbf{I} is the identity tensor, and T is the temperature. Equations for electric forces are derived in literature by applying the divergence operator to \mathbf{T}_e [1].

2. 1. Calculation of the dielectric force

Five expressions were used (separately) for defining the dielectric force.

One of the options was to use the divergence operator built in the software, that is the following equation was used (*cf.* [1]):

$$\mathbf{F}_{\text{diel}} = \nabla \cdot \left(-\frac{1}{2}\varepsilon|\mathbf{E}|^2\mathbf{I} \right) \quad (3)$$

It was also possible to use the equation that is derived after applying the divergence operator (*cf.* [1]), that is the following equation [27,18] (*cf.* [25]):

$$\mathbf{F}_{\text{diel}} = -\frac{1}{2}|\mathbf{E}|^2\nabla\varepsilon \quad (4)$$

A variant of the previous equation that uses cell face values was also investigated:

$$\mathbf{F}_{\text{diel}} = R \left(-\frac{1}{2} (|\mathbf{E}|^2)_f [\mathbf{n}_f \cdot (\nabla \varepsilon)_f] |\mathbf{S}_f| \right) \quad (5)$$

where R is the reconstruction function (see below), \mathbf{n} is the normal unit vector, \mathbf{S} is the surface area vector, subscript f denotes the cell face.

As another option, the expression without the electric field strength was used:

$$\mathbf{F}_{\text{diel}} = R \left(-\frac{1}{2} |\mathbf{n}_f \cdot (\nabla \phi)_f|^2 [\mathbf{n}_f \cdot (\nabla \varepsilon)_f] |\mathbf{S}_f| \right) \quad (6)$$

where ϕ is the electric potential.

The last option was to use the expression that incorporates the electric permittivity (cf. [10]):

$$\mathbf{F}_{\text{diel}} = \frac{R \left\{ -\frac{1}{2} \varepsilon_f (\mathbf{n}_f \cdot (\nabla \phi)_f)^2 [\mathbf{n}_f \cdot (\nabla \varepsilon)_f] |\mathbf{S}_f| \right\}}{|\varepsilon|^2} \quad (7)$$

2. 2. Calculation of the electric field strength

For calculating the electric field strength, at first one of the following equations was used [27]:

$$\mathbf{E} = -\nabla \phi \quad (8)$$

or its variant that uses the cell face values:

$$\mathbf{E} = R \{ -[\mathbf{n}_f \cdot (\nabla \phi)_f] |\mathbf{S}_f| \} \quad (9)$$

or the expression that uses the electric permittivity (cf. [10]):

$$\mathbf{E} = \frac{R \{ -\varepsilon_f (\mathbf{n}_f \cdot (\nabla \phi)_f) |\mathbf{S}_f| \}}{\varepsilon} \quad (10)$$

One equation that could not be directly used is the equation that can be obtained from vector identities (e.g. [28]) [1]:

$$\nabla \times \mathbf{E} = 0 \quad (11)$$

However, this equation can be used indirectly, the curl of the electric field strength can be calculated for controlling the simulation quality. If a curl of the electric field strength is noticed, in order to reduce the numerical error, it was assumed that Helmholtz's vector decomposition (e.g. [29]) can be used, so that:

$$\mathbf{E} = -\nabla \phi + \nabla \times \mathbf{E}_A \quad (12)$$

where \mathbf{E}_A is the artificial solenoidal component of the electric field strength. \mathbf{E}_A was calculated by using the equation:

$$\nabla^2 \mathbf{E}_A = -\nabla \times \mathbf{E} \quad (13)$$

After calculating \mathbf{E}_A , it was possible to optionally correct the electric field strength calculated by Eqs. (8)-(10) in the following way:

$$\mathbf{E} = \mathbf{E}_{\text{unc}} - \nabla \times \mathbf{E}_A \quad (14)$$

where \mathbf{E}_{unc} is the uncorrected electric field strength.

2. 3. Calculation of the electric potential

The electric potential was calculated by using one of the three following ways. The first was to use the equation [17,18]:

$$\nabla \cdot (\varepsilon \nabla \phi) = 0 \quad (15)$$

The second option was to use the expression that incorporates a possible numerical error in the electric field strength calculation:

$$\nabla \cdot (\varepsilon \nabla \phi) = \nabla \cdot (\varepsilon \nabla \times \mathbf{E}_A) \quad (16)$$

Finally, the third approach was to use the following expression:

$$2\nabla \cdot (\varepsilon \nabla \phi) = -\nabla \cdot (\varepsilon \mathbf{E}_{\text{unc}}) \quad (17)$$

\mathbf{E}_{unc} should be important in cases where both Eqs. (14) and (17) are used together because there is a possibility that the former would reduce the improvement that could be obtained by the latter. Eq. (17) incorporates the electric field strength, which should remove one term on the left-hand side and after that leave the numerical error (present in itself) on the right hand side of the Eq. (17).

An optional usage of a recursive loop within the same time step was enabled for cases where either \mathbf{E} or \mathbf{E}_A would otherwise have to be taken from the previous time step.

2. 4. Calculations of the other parameters

The electric permittivity was calculated based on the following equation that is usual for the VoF method and by which newly added fluid properties were handled:

$$\varepsilon = \alpha_1 \varepsilon_1 + \alpha_2 \varepsilon_2 \quad (18)$$

where α is the volume fraction, while subscripts 1 and 2 denote fluid 1 and fluid 2, respectively.

Expressions used for handling of two different fluids that were already present in the starting solver were not modified.

A reconstruction function is a function that reconstructs a cell center value from face values. The reconstruction function built in the OpenFOAM® software was used (*cf.* [30]):

$$R(z_f) = \left(\sum_f \mathbf{S}_f \frac{\mathbf{S}_f}{|\mathbf{S}_f|} \right)^{-1} \cdot \left(\sum_f z_f \frac{\mathbf{S}_f}{|\mathbf{S}_f|} \right) \quad (19)$$

where z is a variable.

In the starting solver that is already present in the OpenFOAM® software, length of time steps can be determined by using the Courant number (Co) and the interface Courant number (iCo). It was decided to add a similar number that could be connected to electrical forces. An equation for the electric Courant number (Co_{el}) can already be found in literature [31], but different equation can be derived by dimensional analysis from the Alfvén-Courant number (ACo) (*cf.* [32]):

$$ACo = \frac{\frac{|\mathbf{B}|}{\sqrt{\mu_0 \rho}}}{\frac{\delta x}{\delta t}} \quad (20)$$

where \mathbf{B} is the magnetic flux density, μ_0 is the vacuum magnetic permeability, x is an axis. It can be seen that:

$$\left[|\mathbf{B}| \sqrt{\frac{1}{\mu_0 \rho}} \right]_{SI} = \frac{m}{s} = \left[|\mathbf{E}| \sqrt{\frac{\varepsilon_0}{\rho}} \right]_{SI} \quad (21)$$

After substituting vacuum by a fluid or fluids, the following expression can be derived:

$$Co_{el} = \frac{|\mathbf{E}| \sqrt{\frac{\varepsilon}{\rho}}}{\frac{\delta x}{\delta t}} \quad (22)$$

An expression for the interface electric Courant number (iCo_{el}) can also be derived from the electric Courant number and the interface Courant number.

During simulations, time steps were determined by using: the Courant number, the interface Courant number, the electric Courant number, and the interface electric Courant number.

3. RESULTS AND DISCUSSION

A system consisting of two fluids with identical densities and kinematic viscosities (10^3 kg m^{-3} and $10^{-6} \text{ m}^2 \text{ s}^{-1}$, respectively), and different electric permittivities ($2 \times 10^{-8} \text{ F m}^{-1}$ and $2 \times 10^{-9} \text{ F m}^{-1}$ for fluids 1 and 2, respectively) was considered in calculations. The interfacial tension between fluids was given a value equal to 0.1 N m^{-1} . In order to remove the effect, which was not of primary interest, the gravity acceleration was neglected. Fluids are situated between two walls with fixed electric potentials (ϕ_{w1} at the wall 1, and $\phi_{w2} = 0 \text{ V}$ at the wall 2).

The IC scheme was used for calculating volume fractions. Meshes were static, unless stated otherwise. The computed results were displayed using ParaView (Kitware, USA) (and paraFoam, OpenFOAM®). The target maximum

value was set to 0.1, unless stated otherwise for the Courant number, the interface Courant number, the electric Courant number, and the interface electric Courant number.

The finally obtained set of expressions consisted of Eq. (1) (the Navier-Stokes equation), Eq. (5) or (6) (for the dielectric force), Eq. (8) (for the electric field strength), Eq. (11) (for checking the curl of the electric field strength), Eq. (15) (for the electric potential), Eq. (18) (for the electric permittivity), Eq. (19) (for the reconstruction function), and Eq. (22) (for the electric Courant number).

3. 1. One-dimensional analysis

A simple one-dimensional set-up was used for straightforward and quick comparison of expressions for the dielectric force. The wall 2 was located at the bottom at $x = 0$, the wall 1 was located at the top at $x = 1$ mm, while the domain was discretized with 100 cells. A value equal to 150 V was used for ϕ_{w1} . Fluid 1 was placed at the bottom half of the geometry, while the fluid 2 was in the upper half. The system was simulated for 0.02 s of its proper time. The electric field strength and the electric potential, used in the simulation, were given by Eqs. (8) and (15), respectively.

3. 1. 1. Comparison of different expressions for the dielectric force

The pressure near the interface that was obtained by using Eqs. (3)-(7) is presented in Figure 1. As can be seen, all of the investigated expressions for the electric force in which only volume fields are used (*i.e.* Eqs. (3) and (4)) caused oscillations in the calculated pressure, indicating numerical instabilities. On the other side, the expressions that use cell face values and their reconstruction yielded stable results, with the exception of Eq. (7), which is the only one in which the reconstruction is not the final step in the calculation because of the later division. If the result obtained by using Eq. (3) is compared to the results obtained by using the other mentioned expressions, it can be seen that the areas with lower and higher pressures even switched their places. Due to this finding, Eqs. (3), (4), and (7) for the dielectric force calculations were disregarded. Also, expressions that use cell face values and their reconstruction without additional steps can be recommended for calculation of the dielectric force.

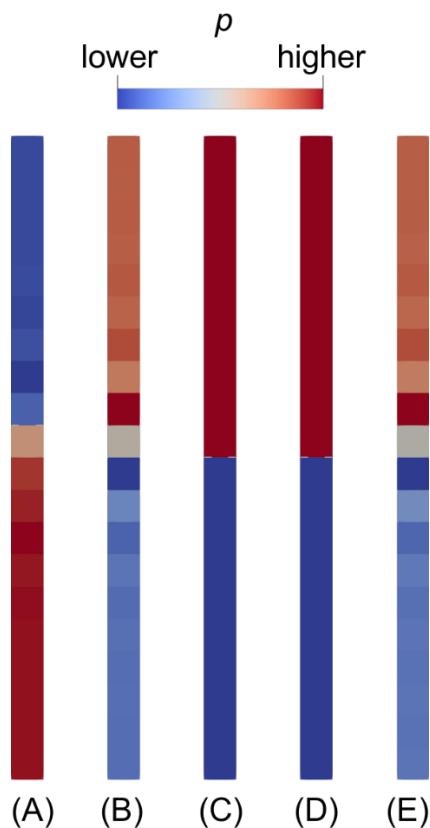


Figure 1. Pressure near the interface (0.4 to 0.6 mm above the bottom wall) at the end of the simulation using various expressions for the dielectric force: A: Eq. (3); B: Eq. (4); C: Eq. (5); D: Eq. (6); E: Eq. (7). This is a qualitative analysis, boundary values of the pressure were adjusted for every simulation independently.

3. 1. 2. Possible improvements by using the electric Courant number

To demonstrate the influence of the electric Courant number and the interface electric Courant number on the results, the velocity magnitude near the interface when either Eq. (4) or Eq. (6) was used is shown in Figure 2 for two cases:

case 1 – the target maximum value for Co , iCo , Co_{el} , and iCo_{el} was 0.1;

case 2 – the target maximum value for Co and iCo was 0.1, while Co_{el} and iCo_{el} did not influence the time step length.

It could be also worth mentioning that in the second case, the whole simulation was performed in one time step because the simulation end time (*i.e.* 0.02 s) was small enough so not to surpass the target maximum value for Co and iCo .

When Eq. (4) was used, the maximum velocity magnitude at the end of the simulation was equal to 0.0690 m s^{-1} for the first case, while it was equal to 0.208 m s^{-1} for the second case. Similarly, when Eq. (6) was used, $7.37 \times 10^{-11} \text{ m s}^{-1}$ was obtained for the first case, while $1.52 \times 10^{-3} \text{ m s}^{-1}$ was obtained for the second case. The fact that the maximum velocity magnitude was higher when Eq. (4) was used can probably be connected to the previously seen oscillations in the pressure for which it was stated that they indicate numerical instabilities. Because it can be said that the velocity magnitude is generally closer to 0 for the case 1, usage of Co_{el} and iCo_{el} for the perfect dielectric model and other models when there is the influence of the electric field could be recommended. Manual time step reduction could also lead to better results. However, it requires several trials, and can lead to a loss of efficiency if overdone.

Certain authors, as [25], use the electric relaxation time for limiting the time step. This approach cannot be used for the perfect dielectric model because the electric conductivity appears in the expression. Also, the Courant number is used for determining the time step instead of the characteristic hydrodynamic time even though it can be found (*e.g.* [1]) and applied to simulations in which there is no electric field, so analogously usage of the electric relaxation time instead of the electric Courant number might not be a suitable option.

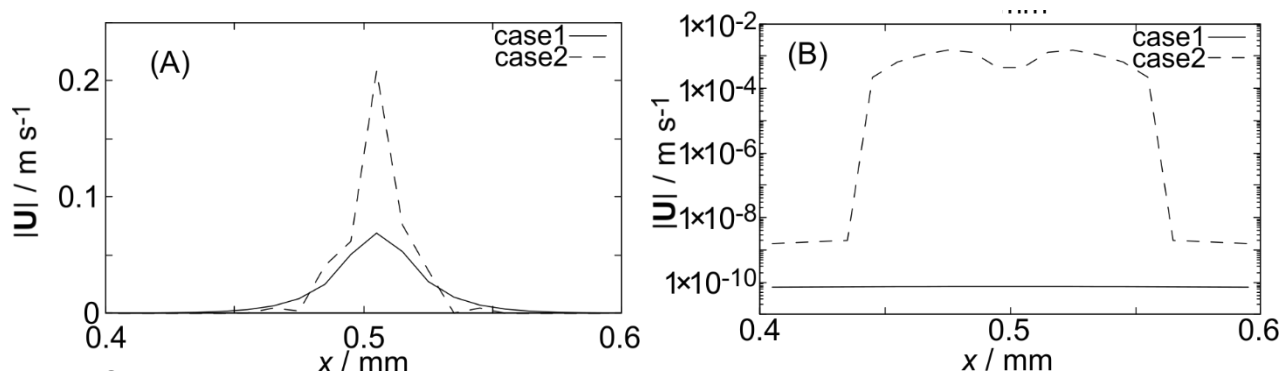


Figure 2. The velocity magnitude near the interface (0.4 mm to 0.6 mm above the bottom wall) at the end of the simulation for case 1 (with Co_{el} and iCo_{el} influence) and case 2 (without Co_{el} and iCo_{el} influence) when either (A) Eq. (4), or (B) Eq. (6) was used

3. 2. Drop analysis

As the second case study, a drop of fluid 1 submersed in the fluid 2 in an external electric field was analyzed.

For this analysis, axially symmetric geometries were assumed as illustrated in Figure 3. At the center of the symmetry axis was a drop of fluid 1. The starting drop radius (r_0) was equal to $2.5 \times 10^{-5} \text{ m}$. On the side opposite to the symmetry axis was the outer surface through which both fluids could exit the geometry, but only the surrounding fluid could enter, and on which the total pressure and the gradient of the electric potential were set to be equal to zero. The distance between the outer surface and the symmetry axis was four times greater than r_0 . The other two sides were walls at a distance from each other five times greater than the starting drop diameter. Static meshes and the starting mesh for the case in which a dynamic mesh was used consisted of prisms on the symmetry axis and hexahedra. It was decided to use 50 cells per the starting drop diameter. When a dynamic mesh was used, the mesh was refined based on α_1 , while the refinement level was set to 1 in the OpenFOAM® software.

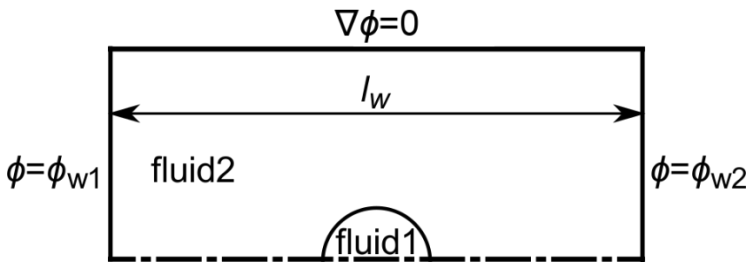


Figure 3. An illustration of the set-up for the drop analysis

3. 2. 1. Curl of the electric field strength

In order to analyze the precision of the numerical procedure, the curl of the electric field strength was considered in the set-up described above using Eq. (5) for the dielectric force. Appearance of this curl signalizes numerical inaccuracy in the calculation. These inaccuracies could be easily overseen when magnetic field effects are also included. The simulation ended at 10^{-8} s, while ϕ_{w1} was equal to 125.7 V.

Different expressions for calculating the electric field strength (i.e. Eqs. (8)-(10)) can be compared based on the value of its curl. Eq. (15) was used for calculation of the electric potential. The curl of the electric field strength at the end of the simulation is shown in Figure 4. The expressions that use cell face values and their reconstruction for calculation of the electric field strength (i.e. Eqs. (9) and (10)) generated very large curl values within the geometry. These values are especially problematic from the point of view of possible future inclusion of magnetic field effects. In contrast, Eq. (8) produced much better results.

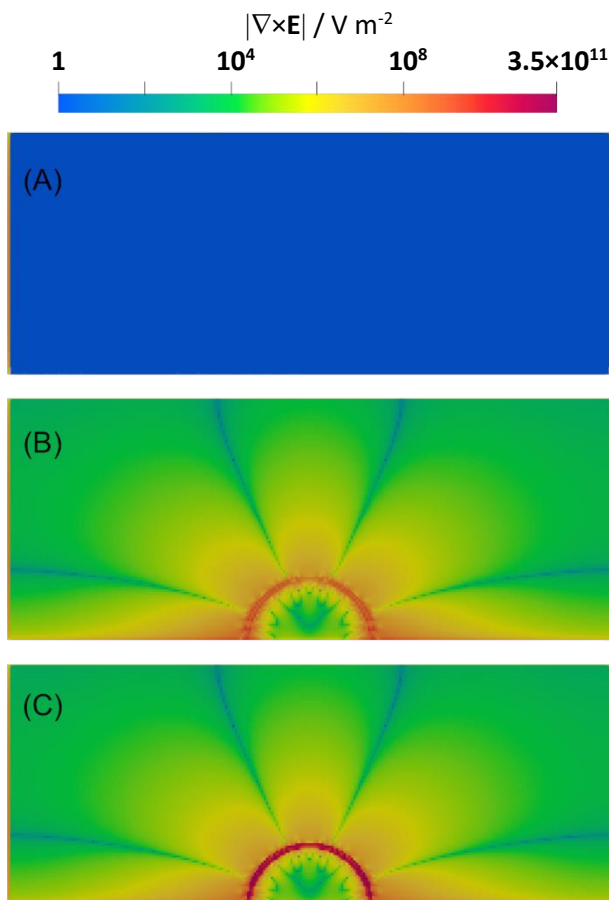


Figure 4. The magnitude of the curl of the electric field strength (when the color map was set to start from 1) at the end of the simulation with the use of Eq. (15) and A: Eq. (8); B: Eq. (9); C: Eq. (10)

If Eq. (9) is used, the mentioned curl can somewhat be reduced by using Eqs. (12)-(14) and (16)-(17), but the reduction is too small. At the end of the simulation, the maximum magnitude of the curl of the electric field was reduced from 4.4×10^9 to 2.5×10^9 V m⁻² when Eqs. (13) and (14) with either Eq. (15) or (17) were used, and to 3.3×10^9 V m⁻² when Eq. (17) was used. On the other hand, the results did not change when Eqs. (13) and (16) either with or without Eq. (14) were used.

Large values of the curl of the electric field strength were also obtained when a dynamic mesh and Eqs. (8) and (15) were used. In this case, the curl maximum magnitude at the end of the simulation was 1.3×10^{12} V m⁻² within the geometry. These analyses lead to the conclusion that the applicability of dynamic meshes, or at least dynamic meshes in the OpenFOAM® software, could be questionable in cases in which the electric field influences fluids, leading also to questionable results if the calculated curl of the electric field strength is not presented.

If Eqs. (8) and (15) and a cell limiter for the gradient of the electric potential are used, large values of the curl of the electric field strength can be also obtained. At the end of the simulation the maximum curl value was 1.3×10^{11} V m⁻² in the interior. This result indicates that the use of limiters for the gradient of the electric potential could be unacceptable. Also, special attention should be paid if magnetic field effects are included, in which case this problem might not be so easily seen.

Based on these findings, use of Eqs. (8) and (15) for calculations of the electric field strength and the electric potential, respectively, could be recommended, while the use of dynamic meshes and limiters of the gradient of the electric potential is not recommended. Also, calculation of the curl of the electric field strength for the perfect dielectric model and other EHD models should be included because otherwise the results could be questionable.

4. CONCLUSIONS

Based on this work several conclusions could be deduced. Inclusion of the calculation of the curl of the electric field strength is recommended, especially if suitability of the model is considered for future inclusion of magnetic field effects. Because of this curl, the expression that uses a value in the cell center could be recommended instead of the ones that use values on the cell faces after analysis, while the applicability of dynamic meshes and limiters of the gradient of the electric field strength was shown to be questionable. Different expressions for calculation of the dielectric force were compared and those that use values on the cell faces showed better results than those that use values in the cell center only. A new electric Courant number was included, in addition to the standard Courant number, in order to improve calculation efficiency and quality of the results, which is expected to be useful in future calculations. It is hoped that inclusion of this new electric Courant number will be valuable in all calculations involving electric fields. By using this work as a basis, a deeper analysis of implementation of the perfect dielectric model and its comparison with the analytical prediction can be performed, which will be the topic of next investigations.

Acknowledgements: This work was supported by the Ministry of Education, Science and Technological Development of the Republic of Serbia (Contracts No. 451-03-9/2021-14/200287 and No. 451-03-9/2021-14/200135) and by Science Fund of the Republic of Serbia (The Program IDEAS MultiPromis 7751519). The authors acknowledge funding provided by the Institute of Physics Belgrade, through the grant by the Ministry of Education, Science, and Technological Development of the Republic of Serbia.

REFERENCES

- [1] López-Herrera JM, Popinet S, Herrada MA. A charge-conservative approach for simulating electrohydrodynamic two-phase flows using volume-of-fluid. *J Comput Phys.* 2011; 230: 1939-1955 <https://dx.doi.org/10.1016/j.jcp.2010.11.042>
- [2] Castellanos A, ed. *Electrohydrodynamics*. Vienna, Austria: Springer-Verlag Wien; 1998 <https://dx.doi.org/10.1007/978-3-7091-2522-9>
- [3] Bošković S, Bugarski B. Review of electrospray observations and theory. *J Eng Process Manag.* 2018; 10: 41-53 <https://dx.doi.org/10.7251/jepm181002041b>
- [4] Singh R, Bahga SS, Gupta A. Electrohydrodynamics in leaky dielectric fluids using lattice Boltzmann method. *Eur J Mech B Fluids.* 2019; 74: 167-179 <https://dx.doi.org/10.1016/j.euromechflu.2018.11.011>
- [5] Shin W-T, Yiacoumi S, Tsouris C. Electric-field effects on interfaces: electrospray and electrocoalescence. *Curr Opin Colloid Interface Sci.* 2004; 9: 249-255 <https://dx.doi.org/10.1016/j.cocis.2004.06.006>

- [6] Pongrác B, Kim H-H, Negishi N, Machala Z. Influence of water conductivity on particular electrospray modes with dc corona discharge – optical visualization approach. *Eur Phys J D*. 2014; 68: 224 <https://dx.doi.org/10.1140/epjd/e2014-50052-4>
- [7] Fernandez de la Mora J, Van Berkel GJ, Enke CG, Cole RB, Martinez-Sanchez M, Fenn JB. Electrochemical processes in electrospray ionization mass spectrometry. *J Mass Spectrom*. 2000; 35: 939-952 [https://dx.doi.org/10.1002/1096-9888\(200008\)35:8<939::aid-jms36>3.0.co;2-v](https://dx.doi.org/10.1002/1096-9888(200008)35:8<939::aid-jms36>3.0.co;2-v)
- [8] Notz PK, Basaran OA. Dynamics of Drop Formation in an Electric Field. *J Colloid Interface Sci*. 1999; 213: 218-237 <https://dx.doi.org/10.1006/jcis.1999.6136>
- [9] Xie J, Wang C-H. Encapsulation of Proteins in Biodegradable Polymeric Microparticles Using Electrospray in the Taylor Cone-Jet Mode. *Biotechnol Bioeng*. 2007; 97: 1278-1290 <https://dx.doi.org/10.1002/bit.21334>
- [10] Thirumalaisamy R, Natarajan G, Dalal A. Towards an improved conservative approach for simulating electrohydrodynamic two-phase flows using volume-of-fluid. *J Comput Phys*. 2018; 367: 391-398 <https://dx.doi.org/10.1016/j.jcp.2018.04.024>
- [11] Bugarski B, Smith J, Wu J, Goosen MFA. Methods for animal cell immobilization using electrostatic droplet generation. *Biotechnol Techn*. 1993; 7: 677-682 <https://dx.doi.org/10.1007/BF00151869>
- [12] Bugarski B, Li Q, Goosen MFA, Poncelet D, Neufeld RJ, Vunjak G. Electrostatic Droplet Generation: Mechanism of Polymer Droplet Formation. *AIChE J*. 1994; 40: 1026-1031 <https://dx.doi.org/10.1002/aic.690400613>
- [13] Poncelet D, Bugarski B, Amsden BG, Zhu J, Neufeld R, Goosen MFA. A Parallel plate electrostatic droplet generator: parameters affecting microbead size. *Appl Microbiol Biotechnol*. 1994; 42: 251-255 <https://dx.doi.org/10.1007/BF00902725>
- [14] Poncelet D, Neufeld RJ, Goosen MFA, Bugarski B, Babak V. Formation of microgel beads by electric dispersion of polymer solutions. *AIChE J*. 1999; 45: 2018-2023 <https://dx.doi.org/10.1002/aic.690450918>
- [15] Manojlovic V, Djonlagic J, Obradovic B, Nedovic V, Bugarski B. Immobilization of cells by electrostatic droplet generation: a model system for potential application in medicine. *Int J Nanomed*. 2006; 1: 163-171 <https://dx.doi.org/10.2147/nano.2006.1.2.163>
- [16] Poncelet D, Babak VG, Neufeld RJ, Goosen MFA, Bugarski B. Theory of electrostatic dispersion of polymer solutions in the production of microgel beads containing biocatalyst. *Adv Colloid Interface Sci*. 1999; 79: 213-228 [https://dx.doi.org/10.1016/S0001-8686\(97\)00037-7](https://dx.doi.org/10.1016/S0001-8686(97)00037-7)
- [17] Supeene G, Koch CR, Bhattacharjee S. Deformation of a droplet in an electric field: Nonlinear transient response in perfect and leaky dielectric media. *J Colloid Interface Sci*. 2008; 318: 463-476 <https://dx.doi.org/10.1016/j.jcis.2007.10.022>
- [18] Munoz CN. Computational modelling of electrohydrodynamic atomization. MSc. Thesis, The University of Manchester, Manchester, UK; 2014.
- [19] Reddy MN, Esmaeeli A. The EHD-driven fluid flow and deformation of a liquid jet by a transverse electric field. *Int J Multiphase Flow*. 2009; 35: 1051-1065 <https://dx.doi.org/10.1016/j.ijmultiphaseflow.2009.06.008>
- [20] Taylor GI. Studies in electrohydrodynamics. I. The circulation produced in a drop by an electric field. *Proc R Soc London, Ser A*. 1966; 291: 159-166 <https://dx.doi.org/10.1098/rspa.1966.0086>
- [21] Moukalled F, Mangani L, Darwish M. The Finite Volume Method in Computational Fluid Dynamics: An Advanced Introduction with OpenFOAM® and Matlab®. Switzerland: Springer International Publishing Switzerland; 2016 <https://dx.doi.org/10.1007/978-3-319-16874-6>
- [22] Andersson B, Andersson R, Håkansson L, Mortensen M, Sudiyo R, Van Wachem B, Hellstrom L. Computational Fluid Dynamics for Engineers. Cambridge, UK: Cambridge University Press; 2012. ISBN: 978-1-107-01895-2
- [23] Li X-g, Fritsching U. Spray Transport Fundamentals. In: Henein H, Uhlenwinkel V, Fritsching U, eds. *Metal Sprays and Spray Deposition*. Cham, Switzerland: Springer International Publishing AG; 2017:89-176 <https://dx.doi.org/10.1007/978-3-319-52689-8>
- [24] Hemida H. OpenFOAM tutorial: Free surface tutorial using interFoam and rasInterFoam. 2008.
- [25] Lima NC. Numerical Studies in Electrohydrodynamics. Ph.D. Thesis, School of Mechanical Engineering of the University of Campinas; 2017.
- [26] Chen C-H. Electrohydrodynamic Stability. In: Ramos A, ed. *Electrokinetics and Electrohydrodynamics in Microsystems*. New York, New York, USA: SpringerWienNewYork; 2011:177-220 <https://dx.doi.org/10.1007/978-3-7091-0900-7>
- [27] Lastow O, Balachandran W. Numerical simulation of electrohydrodynamic (EHD) atomization. *J Electrostat*. 2006; 64: 850-859 <https://dx.doi.org/10.1016/j.elstat.2006.02.006>
- [28] Greenshields CJ. OpenFOAM The Open Source CFD Toolbox: Programmer's Guide Version 3.0.1. OpenFOAM Foundation Ltd.; 2015.
- [29] Davidson PA. Turbulence: An Introduction for Scientists and Engineers. New York, USA: Oxford University Press; 2004. ISBN: 0198529481
- [30] Aguerre HJ, Pairetti CI, Venier CM, Márquez Damián S, Nigro NM. An oscillation-free flow solver based on flux reconstruction. *J Comput Phys*. 2018; 365: 135-148 <https://dx.doi.org/10.1016/j.jcp.2018.03.033>
- [31] Sander S, Gawor S, Fritsching U. Separating polydisperse particles using electrostatic precipitators with wire and spiked-wire discharge electrode design. *Particuology*. 2018; 38: 10-17 <https://dx.doi.org/10.1016/j.partic.2017.05.014>
- [32] Weber N, Galindo V, Stefani F, Weier T, Wondrak T. Numerical simulation of the Taylor instability in liquid metals. *New J Phys*. 2013; 15: 043034 <https://dx.doi.org/10.1088/1367-2630/15/4/043034>

Ispitivanje elektrohidrodinamičkih proračuna

Stefan A. Bošković¹, Aleksandar Karač², Slobodan B. Vrhovac³, Aleksandar Belić⁴ i Branko Bugarski⁴

¹Inovacioni centar Tehnološko-metalurškog fakulteta u Beogradu d.o.o, Beograd, Srbija

²Politehnički fakultet, Univerzitet u Zenici, Zenica, Bosna i Hercegovina

³Univerzitet u Beogradu, Institut za fiziku Beograd, Beograd, Srbija

⁴Univerzitet u Beogradu, Tehnološko-metalurški fakultet, Beograd, Srbija

(Naučni rad)

Izvod

Model idealnog dielektrika je uključen u programski paket OpenFOAM® (OpenFOAM Foundation, UK) i korišćen za ispitivanje i moguće poboljšavanje elektrohidrodinamičkih proračuna. Analizirana su dva različita seta numeričkih simulacija, u kojima su bila modelovana dva različita fluida. Prvi set je bio jednodimenzionalan dok je u drugom setu kap jednog fluida okružena drugim fluidom. U radu je pokazano da se određeni izrazi ili strategije izračunavanja mogu odbaciti usled pojave oscilacija i mogućeg veštačkog stvaranja rotora jačine električnog polja. Korišćenje pokretnih mreža, barem onih prisutnih u programskom paketu OpenFOAM®, i limitera za gradijent jačine električnog polja mogu dovesti do velikih numeričkih grešaka. Takođe je pokazano da bi korišćenje određenih vrednosti sa površi ćelija moglo poboljšati rezultate. Izraz za električni Kuronov broj je izveden dimenzionom analizom i mogao bi se preporučiti za buduće proračune. Očekuje se da su zaključci iz ovog rada prenosivi na druge, komplikovanije modele.

Ključne reči: elektrohidrodinamika; OpenFOAM®; model idealnog dielektrika; električni Kuronov broj